Hindawi
Complexity
Volume 2024, Article ID 1330458, 18 pages
https://doi.org/10.1155/2024/1330458

WILEY | Hindawi

Research Article

Machine Learning-Based Multiagent Control for a Bunch of Flexible Robots

Jun Wang,[1] **Jiali Zhang**,[2] **Jafar Tavoosi**,[3] **and Mohammadamin Shirkhani**[3]

[1]*School of Computer Science and Engineering, Hunan Institute of Technology, Hengyang, Hunan 421001, China*
[2]*School of Engineering, Guangzhou College of Technology and Business, Guangzhou, Guangdong 510800, China*
[3]*Department of Electrical Engineering, Ilam University, Ilam 69315-516, Iran*

Correspondence should be addressed to Jiali Zhang; zhangjiali@gzgs.edu.cn and Jafar Tavoosi; j.tavoosi@ilam.ac.ir

Received 3 May 2023; Revised 2 June 2023; Accepted 20 March 2024; Published 20 April 2024

Academic Editor: Hiroki Sayama

In this paper, two novel methodologies of employing machine learning (here, the type-2 fuzzy system) are presented to control a multiagent system in which the agents are flexible joint robots. In the previous methods, the static mode controller has been investigated, which has little flexibility and cannot measure all the states of the system, but in the method presented in this paper, we can eliminate these disadvantages. The control signal is consisting of feedback from the output and the estimated states of the system. In the first method, the control signal coefficients are calculated from the linear matrix inequality (LMI), followed by a type-2 fuzzy system that adds the compensation signal to the control signal. In the second method, the type-2 fuzzy system is directly used to estimate the control signal coefficients which do not employ LMI. Both methods have their disadvantages and benefits, so in general, one of these two methods cannot be considered superior. To prove the effectiveness of the two proposed methods, a topology with four robots has been considered. Both proposed methods have been evaluated for controlling the angle and speed of the robot link. Also, another simulation was made without using the fuzzy system to verify the importance of our methods. Simulation results indicate the proper efficiency of proposed methods, especially in presence of uncertainty in the system.

1. Introduction

Multiagent systems are the solution to many problems such as horizon facing humans. These types of systems have many advantages over conventional and mono-operating systems, including that working in most situations. This means that because they do not have a single thinking brain and the decision-making is distributed among the agents, even in case of partial failure, they will continue to work. Agent-based systems facilitate parallel processing, parallel processing means that instead of using one processor to perform a task with high computations and heavy processing, the task will be broken into smaller processes with less computational usage [1–4]. Recently, the analysis and control of synchronous behavior of robotic multi-agent systems have been an interesting topic for researchers. An agent is defined as any object that is understandable by using the environment sensor and affected by the stimulus on it can be considered an agent [5–9] such as an intelligent robot equipped with a camera as a sensor and wheels as a stimulus and a manipulator performing specific operations on a workpiece. Many practical applications must have multiple agents working together to pursue a more common purpose while accomplishing their independent objectives. This kind of group with the mentioned features forms a multiagent system [10, 11].

Controlling cohort robots as an example of multiagent systems is one of the most challenging topics in robotics. Complex and challenging operations that may be performed with an enormous, expensive, high degree of freedom, and complex design robot can be achieved with the cooperation of a group of small and similar robots [12–14]. The assembly of parts with complex geometry is an aspect of showing the importance of collaboration in robots [15–17]. Despite this

advantage, robotic cohort systems are more challenging to control than a robot; in these systems, the dynamic equations of the set of robots concerning each other create interactions. The volume of relationships increases and leads to more complex control problems [18–20].

The scope of application of manipulators in various operations is increasing, and the broadening of research and studies in this field is an excellent example of this fact [21–23]. These operations include assembly, welding, cutting, dyeing, crane links, atomic microscope, and the defense and security industries. The future is expected to see the use of powerful manipulators in space exploration and complex subsea operations in the oceans. Manipulators are divided into flexible and rigid categories in terms of design, material, and type of operation. In a flexible manipulator, the dynamics of the link or joint are elastic. The high acceleration of the link movement and its light, long, and narrow material are the two reasons that cause the component to be elastic and its direction deviation during work. The elasticity of the link causes more deviations and vibrations, increases the sitting time, and reduces the accuracy of the position of the grasp (clamp or end toe of the manipulator) [24–26]. Complicating the governing equations and adding severe nonlinear effects make it more difficult for these manipulators to accurately identify and control the design. In fact, of these problems, the benefits of link flexibility in some applications are significant [27, 28]. Increased load-carrying capacity, reduced energy consumption and no need to use high-consumption actuators, cheaper manipulators, faster acceleration in link movement, increased user efficiency due to the use of light links, and safer use due to low link inertia are the benefits. The important thing is the manipulator with a flexible link [29, 30]. Flexibility in the joints is often due to the elastic properties of the motor shaft and power transmission elements from the motor to link or from component to link, such as the gearbox, belt, and pulley. Any manipulator has flexible joints, and the assumption that the joint is rigid is merely a simplifying assumption. From a modeling perspective, the internal curvature and torsion between the actuator and the link are modeled with a torsional spring [31]. The base of the manipulator can also be rigid or flexible. The pros and cons of the base elastic type were presented in [32]. The effect of flexibility in joints has more appearance when the robot moves with high velocity and acceleration and carries a heavy load. Due to design and application type, a manipulator can have rigid or flexible dynamics. Its dynamics will be flexible if, in an application, the manipulator is constructed for transportation as required or works in a slight domain and with high acceleration. However, a large-scale industrial manipulator, in which the accuracy of the position of the grasp is very important and works with heavy loads, is made rigid [33].

Sometimes, in multiagent systems, it is required that agent's concurrence in a certain quantity that is dependent on their states, and eventually, corresponding agents' states converge to an identical vector. For instance, in industry, lifting an object or embarkments of a large piece requires that the manipulators have similar positions. This problem in multiagent systems has been known as consensus. There is no coordination in this state, and the agents are concurrence in case of the final value of their conditions, but also in another state, there is an agent as a leader and other agents follow it. The second state is used when multiple manipulators are far apart, and when the operator adjusts one of the robots, the farther robots also follow its position and states. Other consensus applications in multiagent systems include controlling the arrangement of robotic systems and arranging the motion of satellites. The consensus problem for any multiagent system is that it requires modeling agents, their communication network, and the use of appropriate control law. This rule is adopted based on the specific characteristics of the control agents and objectives\constraints created by the system environment. In most of these methods, problem constraints are represented as matrix inequalities in the design process, and how they are solved plays an essential role in determining the values of the controller [34–38].

It is inevitable to extract the robots' equation of motion to dynamic simulation and controller design. It is commonly done manually in manipulators with restricted links [39]. Modeling and control of different manipulators with various degrees of freedom are presented in [40]. A single-link manipulator with a flexible joint has a nonlinear model but a Lipschitz form. There are multiple papers regarding regulative control and solving a consensus problem for Lipschitz systems [22]. In [41], assuming that the Lipschitz condition is met for the nonlinear term of each agent, and using the Lyapunov stability theory, the static feedback controller is designed to guarantee consensus without a leader. Absolute inequality is also in the form of linear matrix inequalities. In this paper, the performance design of H∞ in the presence of environmental noise has also been investigated. In [42], consensus without a leader has been formatted for a situation in which agents intermittently, not continuously, receive each other information. The designed controller is still the state feedback. By virtue of the abovementioned and many other references, utilization of the Laplacian matrix has the most important in the proposed algorithm. One of the methods that worked for consensus in linear multiagent systems that interact with each other in the form of decentralized is the output feedback [43–45]. For consensus without a leader in linear multiagent systems, the design of a decentralized controller for dynamic output feedback is in the working plans. In addition to the restriction of the agent's linearization, the creation of the controller also leads to the solving of the Bilinear matrix inequalities, and a repetitive homotopic method has been adopted [46–48]. Numerical calculations in bilinear matrix inequalities are much more complex and to solve these inequalities categories, there is no effective algorithm that includes all the forms [49–51]. In [52], the problem of designing the output feedback controller for extensive-scale systems with nonlinear uncertainty has been investigated. To transform bilinear matrix inequalities to linear matrix inequalities and their explicit solution with software, an evolutionary method has been proposed.

Considering the existing challenges to control flexible multiagent robots, as well as the ability to measure and control all system states, a control method is needed. In this paper, the design problem of a dynamic output feedback controller to guarantee consensus, which was previously

designed for linear systems, has been generalized to Lipschitz nonlinear systems. Unlike previous works, the configuration of the problem and design, in a way that selects the order of controller, is in the authorization of the designer and can easily compare the result of a different order of controllers and pick the ideal case. Meanwhile, the final matrix inequality is linear and could determine the controller parameters using implemented efficient algorithms in the existing software. Consensus in the single-link manipulator with flexible joint has been investigated in the previous works using a static state feedback controller. Therefore, all system states should be measured, i.e., an observer should be designed to extract the states. As the output feedback controller is more practical than the mode feedback and more flexible of the dynamic controller than the static one, in this paper, the dynamic output feedback controller has been selected to design. The main contributions of this paper are as follows:

(1) Design of a dynamic output feedback controller for nonlinear Lipschitz systems to ensure consensus
(2) Using linear matrix inequality (LMI) to determine control signal coefficients
(3) Presenting a type-2 fuzzy method to control a multiagent system
(4) Examining the results and proving the effectiveness of the proposed control method

In the second section, the required prerequisites have been presented in the following. The third section introduces a single-link manipulator with a flexible joint, and the decentralized fixed-order output feedback controller is designed for consensus without a leader. The fourth section investigates the numerical example of this system and compares it against other state of the art. Finally, the results and the conclusion of the work have been presented.

2. Mathematical Descriptions

This section presents the required math introductions for the problem statement in brief.

2.1. The Used Symbols. The $x \in R^m$ term introduces a real column vector of m member; the $\otimes$ symbol expresses the Kronecker multiplied between two matrices. The I_n term is the identity matrix and the * symbol is used in the matrix arrays, indicating the transpose of the symmetric array of that member relative to the main diagonal. Also, for the symmetric matrix A, the $A > 0$ symbol means the positive deterministic of that. The $\|0\|$ term introduces the matrix norm and diag (A, B) expresses the diagonal block matrix created from A and B.

2.2. Expressing the Multiagent Systems Using the Graph Theory. To illustrate the distribution of multiagent systems, internal connections, and their network topology, directional graphs are used. This graph shows each agent with one node and the relation between each pair of an agent with one edge. A directional graph with N node is introduced with $g = (V, E, A)$ that $V = (v_1, v_2, \ldots, v_N)$ is the set of nodes and $E \subseteq V \times V$ is the set of edges. The existence of (v_i, v_j) edge in the graph expresses the receiving information of the agent v_j via v_i. In this model, $A = [a_{ij}] \in R^{N\times N}$ is the adjacency matrix. If agent i receives the notification of agent j (the directional edge from j to i would have existed), $a_{ij} > 0$; otherwise, $a_{ij} = 0$ is assumed $(a_{ii} = 0)$.

A neighboring set of an agent is shown with N_i. The member of this set for the agent number i are the agents that receive their information: $N_i = \{v_i \in V, (v_j, v_i) \in E\}$ [14].

2.3. Laplacian Matrix and Important Properties. By investigating the Laplacian matrix with a corresponding network, it is possible to understand the properties of the corresponding network graph and its agent's relation. Laplacian matrix $L = [l_{ij}] \in R^{N\times N}$ related to the diagram of $g = (V, E, A)$ is defi ned in the following equation [17]:

$$\begin{aligned} l_{ij} &= \sum_{j\in N_i} a_{ij}; \\ l_{ij} &= -a_{ij} \\ &\forall i \neq j;\ i, j = 1, \ldots, N. \end{aligned} \tag{1}$$

For the formation of the Laplacian matrix, a_{ij} in the case of being nonzero, each number can be assumed. One of the essential features of the Laplacian matrix is the imperfection of its order ($N-1$ order). That means the zero number will be its eigenvalue surely. The eigenvector corresponding to the eigenvalue of zeros is the unit vector $(1 = [1, 1, \ldots, 1]^T)$.

Graph g is a spanning tree, if and only if the Laplacian matrix has only one eigenvalue of zero and all other values have the positive real part. The smallest nonzero eigenvalue of the Laplacian matrix of graph g is called the second eigenvalue and is shown with $\lambda_2(L(g))$. It is proved that the second eigenvalue indicates the amount of the graph associative. In other words, the larger the second eigenvalue means the more edge number in the graph and the denser the network.

A subgraph tree without a loop is from the main graph, and each node has only one input edge, except for one node that has no input and is named the tree root. A graph includes a spanning tree if a subset of its edges can be found to form a tree that consists of all nodes [53–55]. It should be noted that the necessary condition for the understanding of consensus in a multiagent system is the presence of at least one spanning tree in the connection graph of agents [56–58].

2.4. Consensus Based on the Laplacian Matrix. As mentioned before, the number zero is certainly the eigenvalue of the Laplacian matrix, and the unit vector is the corresponding eigenvector [59–61]. In this section, by considering a simple model for each agent, the basis of the consensus based on the Laplacian matrix is shown. The dynamics of each agent in a multiagent system are assumed in the case of the following equation:

$$\dot{x} = u_i, \quad i = 1, \ldots, N, \tag{2}$$

where x is the position of each agent, u is the controller output, and N is the number of agents in the multiagent system. System (2) is called an integrator.

The problem of consensus in states indeed means finding the appropriate us that due to the agent itself information and neighbor agents, the corresponding states of all agents are moved to an equal value. The problem of consensus in states indeed means finding the appropriate use that due to the agent itself information and neighbor agents, the corresponding states of all agents are moved to an equal value, which can be seen in the following equation:

$$\lim_{t\longrightarrow\infty} |x_i(t) - x_j(t)| = 0, \quad \forall i \neq j. \tag{3}$$

The controller law is proposed in the form of the following equation:

$$u_i = \sum_{j\in N_i} \left(x_j - x_i\right). \tag{4}$$

Its idea is to reduce the difference between the intended agent state with its neighbors.

If $X = [x_1 x_2 \ldots x_N]^T$ and $U = [u_1 u_2 \ldots u_N]^T$ are considered, due to the definition of the Laplacian matrix in equation (1), the controller law of equation (4) is changing to the following equation:

$$U = -LX, \tag{5}$$

and the closed-loop system in this state is converting in the form of the following equation:

$$\dot{X} = -LX. \tag{6}$$

Since the eigenvalues of the Laplacian matrix corresponding with a single-piece graph is continuously negative, the $-L$ eigenvalues are consistently nonpositive and the system is stable [20]. Therefore, $\lim_{t\longrightarrow\infty}\dot{X} = 0$ and in consequence, $\lim_{t\longrightarrow\infty}\mathrm{LX} = 0$. The final values of the X vector are assumed in the case of $X^* = [x_1^* x_2^* \ldots x_N^*]^T$. Thus, it can be said that $LX^* = L[x_1^* x_2^* \ldots x_N^*]^T = 0$. Based on the Laplacian matrix characteristics, the unit vector is its eigenvector. It means that $L(c[1, \ldots, 1]^T) = 0$ and $X^* = c[1, \ldots, 1]^T$. The number c is the consensus value [21].

Method 1 [22]: a result from S-procedure: suppose two symmetrical and codimensional matrices of T_0 and T_1. It is assumed that equation (7) for those two is determinate.

$$\zeta^T T_1 \zeta \geq 0, \zeta^T T_0 \zeta > 0, \quad \forall \zeta \neq 0. \tag{7}$$

If there is a $\tau \geq 0$ in a way that $T_0 - \tau T_1 > 0$, then the assumption in equation (7) is determinate and vice versa.

Method 2 [15]: Schur complement: the Schur complement method converts many nonlinear inequalities in the form of equation (8) to linear matrix inequalities.

$$R(x) > 0, Q(x) - S(x)R^{-1}(x)S^T(x) > 0, \tag{8}$$

where $R(x)$ and $Q(x)$ both are symmetrical matrices, and the Schur complement converts the inequalities of equation (8) to the following linear inequalities:

$$\begin{pmatrix} Q(x) & S(x) \\ * & R(x) \end{pmatrix} > 0. \tag{9}$$

3. Problem Statement and Output Feedback Controller Design

In this section, the consensus in a multiagent system consisting of flexible joint robot will be investigated while introducing the dynamic of the single-link robot with a flexible joint. In Figure 1, the experimental plan of a robotic link with a single degree of freedom and flexible joint has been shown [41].

In Figure 2, the angular rotation direction of the engine and link, the modeling of the joint with a torsional spring, and the link's general performance are considered [25].

By using the governing laws in physics, the dynamic of each agent can be stated in the form of the following equation [42]:

$$\begin{aligned} J_l\ddot{\theta}_l + mgl\sin(\theta_l) + k(\theta_l - \theta_m) = 0, \\ J_m\ddot{\theta}_m + k(\theta_m - \theta_l) + B\dot{\theta}_m = K_\tau u, \end{aligned} \tag{10}$$

where k is the spring constant, K_τ is determined efficiency, J_m and J_l are the inertia of the engine and link, respectively, u is the controlling input vector, B is the bearing friction, and m and l are the mass and the half-link length, respectively. In this manipulator, if the link works at the horizontal state and has no height change, its model becomes entirely linear; but in practice, the application of the vertical state is more. By the definition of angular velocity as an angular position derivative, the first-order equations are obtained as follows:

$$\begin{aligned} \dot{\theta}_m &= \omega_m, \\ \dot{\omega}_m &= \frac{k}{J_m}(\theta_l - \theta_m) - \frac{B}{J_m}\omega_m + \frac{K_\tau}{J_m}u, \\ \dot{\theta}_l &= \omega_l, \\ \dot{\omega}_l &= -\frac{k}{J_m}(\theta_l - \theta_m) - \frac{mgh}{J_l}\sin(\theta_l). \end{aligned} \tag{11}$$

According to equation (11), the i^{th} model of a robot in a multiagent system with N agent is expressed in the following equation:

$$\begin{aligned} \dot{x}_i &= Ax_i + Bu_i + h_i(x), \quad i = 1, \ldots, N, \\ y_i &= Cx_i. \end{aligned} \tag{12}$$

In system (11), $x_i = (\theta_m^T \omega_m^T \theta_l^T \omega_l^T)^T \in R^4$ is the states vector of each robot, $h_i(x) = (000 - (mgh/J_l)\sin(\theta_l))^T$ is the nonlinear sentence of each robot, and

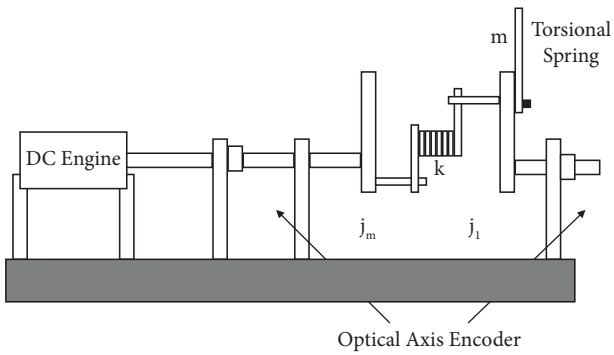

Figure 1: Plan of the single-link robot with flexible joint.

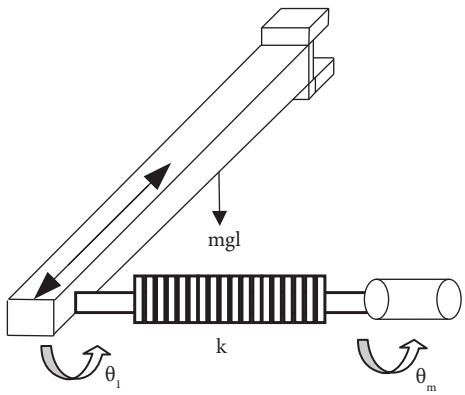

Figure 2: Schematic sketch of the single-link robot with flexible joint.

$B = (0(K_\tau/J_m)00)^T$. In this system, two separate outputs of ω_m and θ_m are defined as $C = \begin{pmatrix} 1 & 0 & 0 & 0 \\ 0 & 1 & 0 & 0 \end{pmatrix}$.

A system that is expressed in the form of equation (12) and satisfies the below condition is called in terms of the Lipschitz nonlinear system [11].

$$\|h(x) - h(y)\| \le \omega \|x - y\|, \quad \forall x, y \in R^n, \tag{13}$$

where $\omega > 0$ is the Lipschitz constant. There are many advantages to designing controllers for systems in this form. Methods based on linear matrix inequalities for the design of resistant dynamic feedback controllers or linear observers can be easily implemented for such systems. Also, many linear systems subjected to a network working together have unidentifiable mutual effects on each other. By modeling each subsystem to a form of equation (12), the robustness of the whole system can be guaranteed compared to mutual effects [25].

In general state, $h(x_i)$ is a linear piecewise vectorized function towards both t and x_i arguments that satisfy equation (14) in the association field.

$$h_i(t, x_i)^T h_i(t, x_i) \le \overline{\alpha}_i^2 x_i^T \left(\overline{H}_i^T \overline{H}_i \right) x_i. \tag{14}$$

In equation (14), $x_i \in R^n$ and $\overline{H}_i$ is a $n \times n$ known matrix. $\overline{\alpha}$ is also the maximum bound that established equation (14).

As mentioned, the consensus problem is the means of a controller design that can converge the agent's states to a standard vector due to the agents' relation manner with each other. As mentioned, the consensus problem is the means of a controller design that can converge the agent's states to a standard vector due to the agents' relation manner with each other as shown in the following equation [14]:

$$\lim_{t \longrightarrow \infty} \| x_i(t) - x_j(t) \| = 0, \quad \forall i \ne j. \tag{15}$$

To accomplish the consensus following equation (15), first, all of the existing agents to a form of equation (12), in an N agent system, in the form of the unit system but with a large dimension is expressed as in the following equation:

$$\begin{aligned} \dot{x} &= A_D x + B_D u + h(x), \quad x \in R^{4 \times N}, u \in R^N, \\ y &= C_D x, \quad y \in R^{2 \times N}. \end{aligned} \tag{16}$$

In equation (16), $x = [x_1^T, x_2^T, \ldots, x_N^T]^T$ exemplifies the state vector of the whole system, $u = [u_1^T, u_2^T, \ldots, u_N^T]^T$ is a vector of controller inputs and $h(x) = [h_1(x_1)^T, h_2(x_2)^T, \ldots, h_N(x_N)^T]^T$ is the vector of nonlinear sentences of the entire system, and $y = [y_1^T, y_2^T, \ldots, y_N^T]^T$ is the output vector. Also, $A_D = I_N \otimes A, B_D = I_N \otimes B, C_D = I_N \otimes C$.

Now, $\overline{H}^T = [\overline{H}_1^T, \ldots, \overline{H}_N^T]$ and $\overline{\Gamma} = \text{diag}(\overline{\gamma}_1 I_4, \ldots, \overline{\gamma}_N I_4)$ is considered. It has been shown in [9] that by defining $\overline{\gamma}_i = \overline{\alpha}_i^{-2}$, the H and Γ matrices can consistently be found according to the following equation:

$$h(t, x)^T h(t, x) \le x^T \overline{H}^T \overline{\Gamma}^{-1} \overline{H} \le x^T H^T \Gamma^{-1} H x, \tag{17}$$

where $H = \text{diag}(H_1, \ldots, H_N)$, $\Gamma = \text{diag}(\gamma_1 I_4, \ldots, \gamma_N I_4)$, and $\gamma_i > 0$.

Now, to reach a consensus, the output feedback decentralized controller expressed in [14] is used by n_c constant order equation as follows:

$$\begin{aligned} \dot{\hat{x}} &= \hat{A}_D \hat{x} + \hat{B}_D L_{\overline{C}} y, \quad \hat{x} \in R^{n_c N}, \\ u &= \hat{C}_D \hat{x} + \hat{D}_D L_{\overline{C}} y. \end{aligned} \tag{18}$$

In controller (18), $\hat{x} = [\hat{x}_1^T, \hat{x}_2^T, \ldots, \hat{x}_N^T]^T$ is the set of controller states and $L_{\overline{C}} = L \otimes I_2$. $\hat{A}_D, \hat{B}_D, \hat{C}_D$, and $\hat{D}_D$ have the structure in the following form:

$$\begin{aligned} \hat{A}_D &= \text{diag}\left(\hat{A}_1, \hat{A}_2, \ldots, \hat{A}_N\right), \\ \hat{B}_D &= \text{diag}\left(\hat{B}_1, \hat{B}_2, \ldots, \hat{B}_N\right), \\ \hat{C}_D &= \text{diag}\left(\hat{C}_1, \hat{C}_2, \ldots, \hat{C}_N\right), \\ \hat{D}_D &= \text{diag}\left(\hat{D}_1, \hat{D}_2, \ldots, \hat{D}_N\right). \end{aligned} \tag{19}$$

Theorem 1. *The dynamic output controller of equation (18) conveys the consensus of the defined system in equation (12) if there has been the symmetrical and determined positive matrix of P in the form of equation:*

$$\begin{aligned} P &= \operatorname{diag}(P_1, P_2),\\ P_1 &= \operatorname{diag}(p_{11}, p_{12}, \ldots, p_{1N}),\\ P_2 &= \operatorname{diag}(p_{21}, p_{22}, \ldots, p_{2N}),\\ p_{1i} &\in R^{4\times 4}, p_{2i} \in R^{n_c \times n_c} i = 1, \ldots, N, \end{aligned} \tag{20}$$

and the R, Z, M, Q, H, and Γ matrices of the positive scalar of τ, (equation (21)), as it is confirmed:

$$\begin{pmatrix} L + \tau \begin{bmatrix} H^T \Gamma^{-1} H & 0 \\ * & 0 \end{bmatrix} & P \\ * & -\tau I \end{pmatrix} < 0. \tag{21}$$

In equation (21), $\Gamma = \operatorname{diag}(\gamma_1 I_4, \ldots, \gamma_N I_4)$ and according to equation:

$$\begin{aligned} L &= \overline{A}^T P + P\overline{A} + 2\lambda P\\ &= \begin{bmatrix} A_D^T P_1 + L_C^T C_D^T Q^T + P_1 A_D & L_C^T C_D^T Z^T + M \\ +QC_D L_C + 2\lambda P_1 & \\ * & R^T + R + 2\lambda P_2 \end{bmatrix}. \end{aligned} \tag{22}$$

Also, controller parameters of equation (18) will be computable from equation:

$$\begin{aligned} \widehat{A}_D &= {P_2}^{-1} R,\\ \widehat{B}_D &= {P_2}^{-1} Z,\\ \widehat{C}_D &= \left((P_1 B_D)^T (P_1 B_D) \right)^{-1} (P_1 B_D)^T M,\\ \widehat{D}_D &= \left((P_1 B_D)^T (P_1 B_D) \right)^{-1} (P_1 B_D)^T Q. \end{aligned} \tag{23}$$

Proving: By applying the controller of equation (18) to a defined system in equation (16), the state-space form of a closed-loop system can be written as an equation:

$$\dot{\overline{x}} = \overline{A}\overline{x} + z. \tag{24}$$

Which in that $\overline{x} = [x^T, \widehat{x}^T]^T$, $\overline{A} = \begin{pmatrix} A_D + B_D \widehat{D}_D L_{\overline{C}} C_D & B_D \widehat{C}_D \\ \widehat{B}_D L_{\overline{C}} C_D & \widehat{A}_D \end{pmatrix}$ and $z = \begin{bmatrix} h(t,x) \\ 0_{nN\times 1} \end{bmatrix}$.

So that the dimension of diagonal block Laplacian matrix of $L_{\overline{C}}$ being affected by the number of states of each agent and the nine output of (q), with the below procedure, is substituted by $L_C = L \otimes I_n$:

$$\begin{aligned} L_{\overline{C}} C_D &= \left(L \otimes I_q\right)\left(I_N \otimes C\right) = \left(L I_N\right) \otimes \left(I_q C\right)\\ &= \left(I_N L\right) \otimes \left(C I_n\right) = \left(I_N \otimes C\right)\left(L \otimes I_n\right)\\ &= C_D L_C. \end{aligned} \tag{25}$$

Now, the $\overline{A}$ form is changed to the below form:

$$\overline{A} = \begin{pmatrix} A_D + B_D \widehat{D}_D C_D L_C & B_D \widehat{C}_D \\ \widehat{B}_D C_D L_C & \widehat{A}_D \end{pmatrix}. \tag{26}$$

Presently, so that the system of equation (24) is stable and during the guarantee of stability, the unknown parameters of the controller will also be obtained, by using the below function of square Lyapunov, the standard of Lyapunov stability theorem is defined as an equation.

$$V = \overline{x}^T P \overline{x}. \tag{27}$$

The symmetrical and determined positive matrix of P is assumed in the form of equation (20).

To improve the convergence rate of system states, by defining the positive and desired parameter of λ, the Lyapunov stability theorem is written for convergence of $e^{\lambda t} x(t)$ to zero. Hence, by differentiation from equation (27) and substituting of equations, the system of equation (24) has the form of equation:

$$\begin{aligned} \frac{dV}{dt} &= \frac{d\left(e^{\lambda t}\overline{x}\right)^T}{dt} P\left(e^{\lambda t}\overline{x}\right) + \left(e^{\lambda t}\overline{x}\right)^T P \frac{d\left(e^{\lambda t}\overline{x}\right)}{dt}\\ &= e^{\lambda t}\left[\overline{x}^T\left(2\lambda P + \overline{A}^T P + P\overline{A}\right)\overline{x} + z^T P\overline{x} + \overline{x} P z\right] e^{\lambda t} = e^{\lambda t} \begin{bmatrix} \overline{x} \\ z \end{bmatrix}^T \begin{bmatrix} L & P \\ * & 0 \end{bmatrix} \begin{bmatrix} \overline{x} \\ z \end{bmatrix} e^{\lambda t}, \end{aligned} \tag{28}$$

where L is the term defined in equation (22) so that the closed loop of the system in equation (24) be stable, equation (28) should be determined negative or, in other words; its analogy is the determined positive equation.

$$-\begin{bmatrix} \overline{x} \\ z \end{bmatrix}^T \begin{bmatrix} L & P \\ * & 0 \end{bmatrix} \begin{bmatrix} \overline{x} \\ z \end{bmatrix} \geq 0. \tag{29}$$

Due to the positivity of the scalar of $e^{\lambda t}$, it is eliminated without the effect of the above inequality. Now, due to the

definition of z and based on what is expressed in equations (15) and (30) can be written as below:

$$z^T z \le x^T \left(H^T \Gamma^{-1} H\right) x. \tag{30}$$

The equation (30) can be rewritten in the form of equation (31) matrix:

$$\begin{bmatrix} \overline{x} \\ z \end{bmatrix}^T \begin{bmatrix} \begin{bmatrix} H^T\Gamma^{-1}H & 0 \\ * & 0 \end{bmatrix} & 0 \\ * & -I \end{bmatrix} \begin{bmatrix} \overline{x} \\ z \end{bmatrix} \ge 0. \tag{31}$$

Now, due to equations (29) and (31), and by the use of method 1 (S-procedure), equation (32) is

$$\begin{bmatrix} \overline{x} \\ z \end{bmatrix}^T \begin{bmatrix} \begin{bmatrix} H^T\Gamma^{-1}H & 0 \\ * & 0 \end{bmatrix} & 0 \\ * & -\tau I \end{bmatrix} \begin{bmatrix} \overline{x} \\ z \end{bmatrix} < 0. \tag{32}$$

According to the characterization of the non-linear sentence, an appropriate value for Γ can be found by use of equation (30). The larger values designated do not create any difficulty; the locality of finding controller parameters will be restricted. To establish equations (18) and (32) is required to be signified. End of proving.

Corollary 2. *If the non-linear sentences are not unidentifiable or appear as uncertain, or are effective in the obstructive input environment, the Γ is also unknown. Therefore, the unknown parameters of τ and Γ must be separated from each other till equation (32) become the form of linear matrix inequalities. For this reason, the Schur complimentary technique has been used and the equation (21) rescript in the form of equation:*

$$\begin{bmatrix} L & P & \tau(\mathrm{H}\ 0)^T \\ * & -\tau I & 0 \\ * & * & -\widehat{\Gamma} \end{bmatrix} < 0. \tag{33}$$

In inequalities of equation (33), $\widehat{\Gamma} = \tau\Gamma, \widehat{\Gamma} = \mathrm{diag}\,(\widehat{\gamma}_1 I_4, \ldots, \widehat{\gamma}_N I_4)$. From equation (17), it can be deduced that by minimizing γ_i *s*, the Γ is also minimized. In this manner, the Γ^{-1} and the $\widehat{\Gamma}^{-1}$ are also maximized in consequence. Meanwhile, to obtain the most assured bound for the expression of equation (17), the matrix inequalities of equation (33) are calculated with the aim of minimizing $\sum_{i=1}^{N} \widehat{\gamma}_i$.

4. Proposed Type-2 Fuzzy System

The proposed type 2 fuzzy neural network is shown in Figure 3.

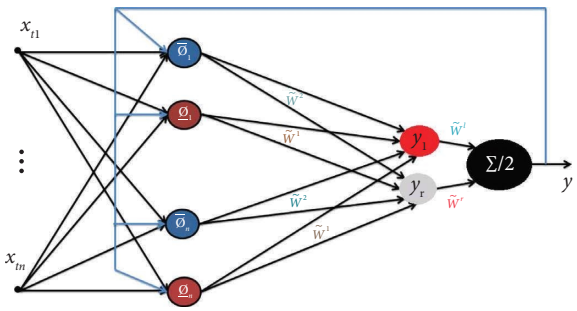

Figure 3: Proposed type 2 fuzzy neural network. (Figure 3 is reproduced from Hesarian et al. [62] [under the Creative Commons Attribution License/public domain]).

Equation (34) represents the calculations of the first layer:

$$\begin{cases} \overline{\varnothing}_{ji}\left(x_j\right) = \begin{cases} \left(x_j - c_{ji}^1\right)^2, & x_j < c_{ji}^1, \\ 1, & c_{ji}^1 \le x_j \le c_{ji}^2, \\ \left(x_j - c_{ji}^2\right)^2, & x_j > c_{ji}^2, \end{cases} \\ \underline{\varnothing}_{ji}\left(x_j\right) = \begin{cases} \left(x_j - c_{ji}^2\right)^2, & x_j \le \dfrac{c_{ji}^1 + c_{ji}^2}{2}, \\ \left(x_j - c_{ji}^1\right)^2, & x_j > \dfrac{c_{ji}^1 + c_{ji}^2}{2}. \end{cases} \end{cases} \tag{34}$$

The upper and lower of the i^{th} neuron and the j^{th} input are denoted by $\overline{\varnothing}_{ji}$ and $\underline{\varnothing}_{ji}$, respectively. Equation (35) represents the output of the first layer.

$$\begin{cases} \overline{\varnothing}_i(x) = \exp\left(-\dfrac{\sum_{j=1}^{n+1} \widetilde{\varnothing}_{ji}\left(x_j\right)}{\sigma_i^2}\right), \\ \underline{\varnothing}_i(x) = \exp\left(-\dfrac{\sum_{j=1}^{n+1} \underline{\varnothing}_{ji}\left(x_j\right)}{\sigma_i^2}\right), \end{cases} \tag{35}$$

where $\overline{\varnothing}_i$ and $\underline{\varnothing}_i$ are the upper and lower of the i^{th} neuron $(i = 1, 2, \ldots, m)$, respectively. $x \in (x_j), j = 1, \ldots, n$ is the input vector, and $c_{ji} \in [c_{ji}^1, c_{ji}^2]$ is the center of all the type-2 fuzzy neurons. Equation (36) represents the endpoints of the second layer.

$$\begin{cases} \widehat{y}_l = \dfrac{\sum_{i=1}^{q} \overline{\varnothing}_i(x) c_{w_i}^2 \sigma_{w_i} + \sum_{i=q+1}^{m} \underline{\varnothing}_i(x) c_{w_i}^1 \sigma_{w_i}}{\sum_{i=1}^{q} \overline{\varnothing}_i(x) \sigma_{w_i} + \sum_{i=q+1}^{m} \underline{\varnothing}_i(x) \sigma_{w_i}}, \\ \widehat{y}_r = \dfrac{\sum_{i=1}^{p} \underline{\varnothing}_i(x) c_{w_i}^1 \sigma_{w_i} + \sum_{i=p+1}^{m} \overline{\varnothing}_i(x) c_{w_i}^2 \sigma_{w_i}}{\sum_{i=1}^{p} \underline{\varnothing}_i(x) \sigma_{w_i} + \sum_{i=p+1}^{m} \overline{\varnothing}_i(x) \sigma_{w_i}}, \end{cases} \tag{36}$$

where p and q are the left and right switching points of the Type-II fuzzy system. Also in this equation, m, w_i, c_{w_i}, and σ_{w_i} are the mean value of the first layer neurons, the weights, the center of weights, and the spread of weights, respectively. Equation (37) represents the general output of the network.

$$\widehat{y} = \frac{1}{2} \frac{\sum_{i=1}^{q} \widehat{y}_r c_{w_i}^r \sigma_{w_i} + \sum_{i=q+1}^{m} \widehat{y}_l c_{w_i}^l \sigma_{w_i}}{\sum_{i=1}^{q} \widehat{y}_r \sigma_{w_i} + \sum_{i=q+1}^{m} \widehat{y}_l \sigma_{w_i}}, \tag{37}$$

where, $\mathbf{c}_{\mathbf{w}_i}^{\mathbf{r}}$ and $\mathbf{c}_{\mathbf{w}_i}^{\mathbf{l}}$ are the centers $\widetilde{\mathbf{W}}^{\mathbf{r}}$ of and $\widetilde{\mathbf{W}}^{\mathbf{l}}$, respectively. As seen in Figure 3 and equations (34) and (35), the proposed type-2 fuzzy system is an investigated radial basis function neural network In fact, our proposed model has two major differences with the existing works: one is the use of type-2 fuzzy membership functions in the hidden layer and the other is the presence of feedback from the output of the neural network to the neurons of the hidden layer. The details and equations of updating the parameters of type-2 fuzzy system are stated in the appendix section.

As mentioned in the abstract, two methods are proposed in this article. In the first method, equation (18) is written in the following form.

$$\begin{aligned} \dot{\widehat{x}} &= \widehat{A}_D \widehat{x} + \widehat{B}_D L_{\overline{C}} y, \\ u &= \widehat{C}_D \widehat{x} + \widehat{D}_D L_{\overline{C}} y + u_{\text{fuzzy}}, \end{aligned} \tag{38}$$

where u_{fuzzy} is calculated by the fuzzy system and according to the amount of error. But in the second method, the parameters of equation (23) are calculated by the fuzzy system, so there is no need to solve LMI.

5. Simulation Results

This section investigates a multi-agent system with three agents to assess the designed method. Each of them is an experimental single-link robot with a flexible joint. All simulations are done in MATLAB/Simulink software environment and this experimental model's parameters have been reported in Table 1. These values are selected according to reference [43].

By substituting the numerical values of parameters, the state space of the system is obtained in equation (34) in the form of equation (12) with A, B, C, and h.

$$\begin{aligned} A &= \begin{pmatrix} 0 & 1 & 0 & 0 \\ -48.6 & -1.25 & 48.6 & 0 \\ 0 & 0 & 0 & 1 \\ 19.5 & 0 & -19.5 & 0 \end{pmatrix}, \\ B &= \begin{pmatrix} 0 \\ 21.6 \\ 0 \\ 0 \end{pmatrix}, \\ h &= \left(\begin{pmatrix} 0 & 0 & 0 & -3.33 \sin \theta_l \end{pmatrix} \right)^T, \\ C &= (10000100). \end{aligned} \tag{39}$$

These three agents with a triangular topology illustrated in Figure 3 relate to each other.

Due to Figure 3 and equation (1), the Laplacian matrix of this system is written in the below form.

$$L = \begin{bmatrix} 1 & 0 & 0 & -1 \\ -1 & 1 & 0 & 0 \\ 0 & -1 & 1 & 0 \\ 0 & 0 & -1 & 1 \end{bmatrix}. \tag{40}$$

Supposing $H = I_{12}$ and $\Gamma = 30000 I_{12}$ for covering the upper bound of a non-linear sentence and also $\lambda = 0.8$ and with simulating the above system in MATLAB and solving the linear matrix inequalities obtained from equation (33) with the YALMIP toolbox, the controller parameters with second-order are extracted.

In Figure 4, the convergence of θ_m and θ_l and in Figure 5 also the convergence of ω_m and ω_l with an exact amount and the establishment of consensus with second-order controller ($n_c = 2$) is observed:

Controlling multi-agent systems on the one hand and controlling robots with flexible joints on the other hand are two challenging issues. It can be clearly seen from Figures 5–8 that the proposed method has a good performance. In the following, both proposed methods are compared with another method (output feedback).

From Figures 9–12, it is clear that both proposed methods have similar performance and perform much better than the output feedback method. To compare the obtained results with similar previous works, an algorithm and the controller used in the [16] for consensus in agents in the form of Lipschitz non-linear has been investigated. The proposed controller in [16] is in the below form:

$$u_j = cK \sum_{j=1}^{N} a_{ij} \left(x_i - x_j \right) \tag{41}$$

Table 1: Specification of the single-link robot with flexible joint.

Robot specification	Symbol	Value	Unit
Actuator interia (DC engine)	J_m	0.0037	kgm^2
Link interia	J_l	0.0093	kgm^2
Engine bearing movement friction	B	0.046	NmV^{-1}
Coefficient of torsional spring constant	k	0.18	Nmrad^{-1}
Efficiency amplifier for control		0.008	NmV^{-1}
Link mass	m	0.21	kg
Half-link length	L	0.3	m
Engine angular rotation	θ_m	State variable	rad
Link angular rotation	θ_l	State variable	rad
Engine angular velocity	ω_m	State variable	$\text{rad}\cdot\text{s}^{-1}$
Link angular velocity	ω_l	State variable	$\text{rad}\cdot\text{s}^{-1}$

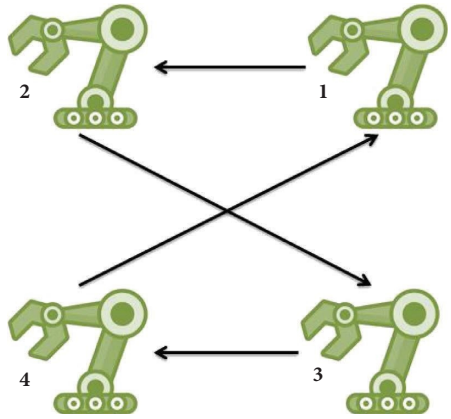

Figure 4: The system of topology network with four agents.

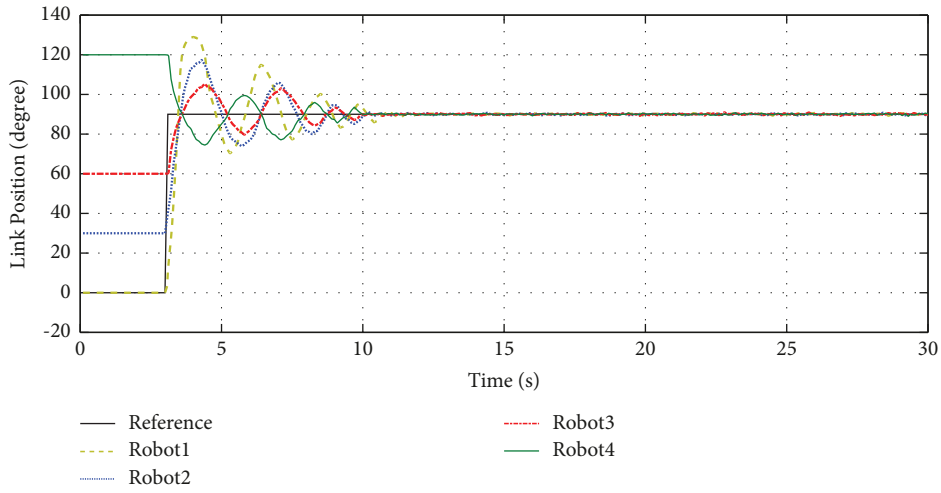

Figure 5: Tracking the reference link position by all 4 robots.

where c and K should be specified, and a_{ij} is related to a network adjacency matrix of agents.

Table 2 shows the comparison of integration of the controller output's area under the curve for four different robots. In Table 3, controller parameters and the nearest pole of a closed-loop system to the imaginary axis are observed as a standard of relative stability. The real value is the nearest pole to the axis in both controllers.

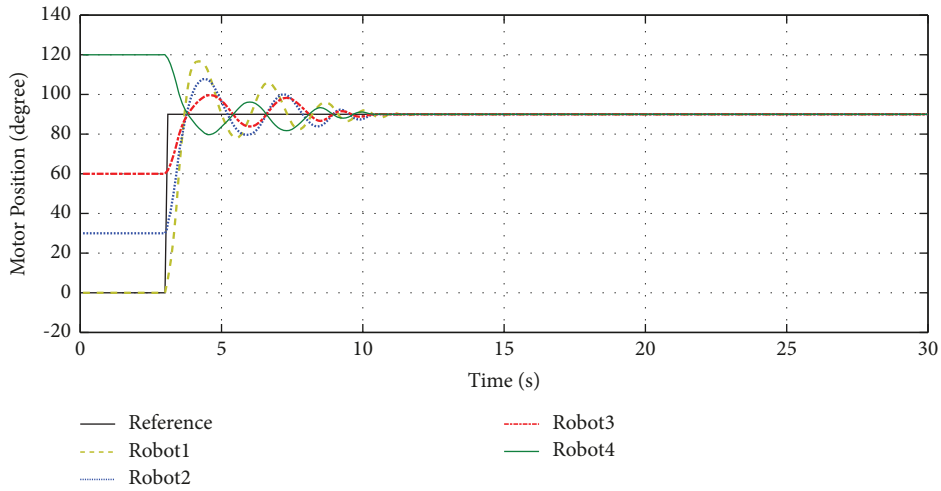

Figure 6: Tracking the reference motor position by all 4 robots.

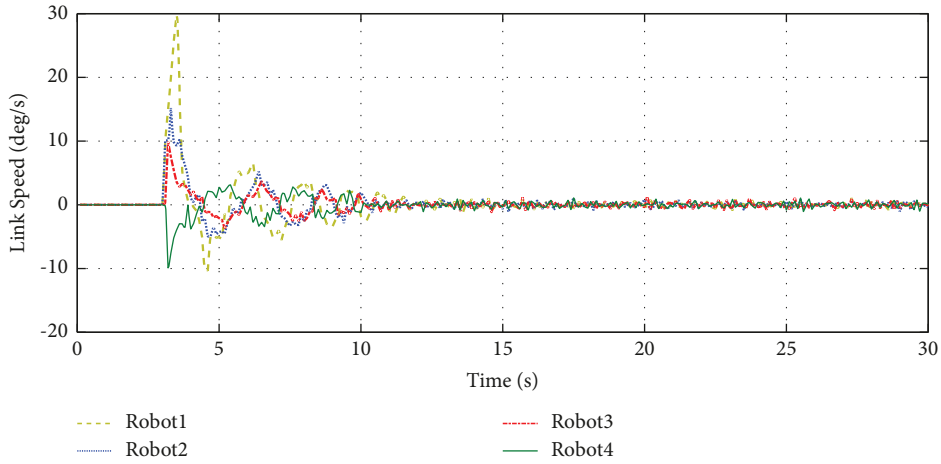

Figure 7: The link speed of the all 4 robots.

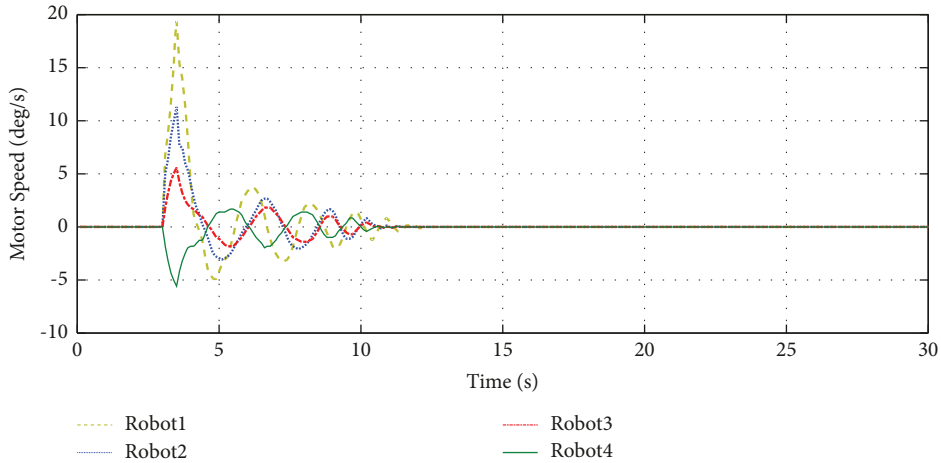

Figure 8: The motor speed of the all 4 robots.

For further comparison with the existing works, Table 4 shows the three criteria of RMSE, settling time and overshoot.

As can be seen in Table 4, both proposed methods have a much better performance than the methods presented in [16, 26].

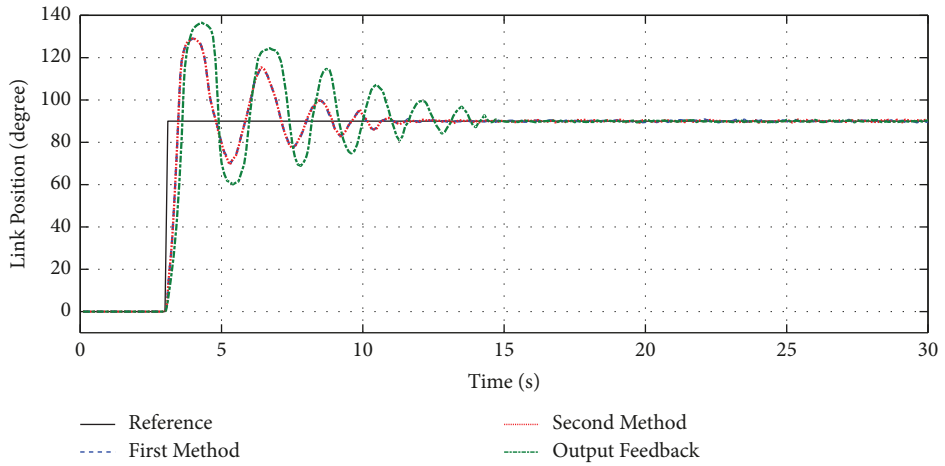

Figure 9: Comparison of both proposed methods with output feedback method in reference link position tracking.

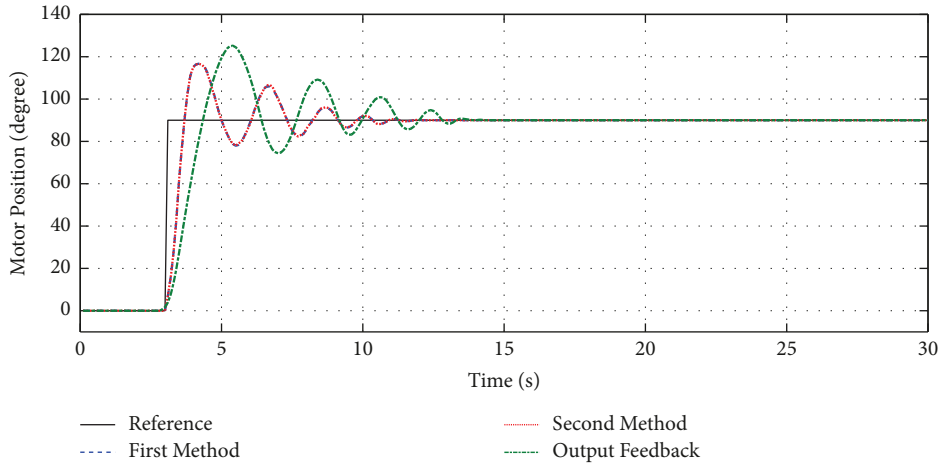

Figure 10: Comparison of both proposed methods with output feedback method in reference motor position tracking.

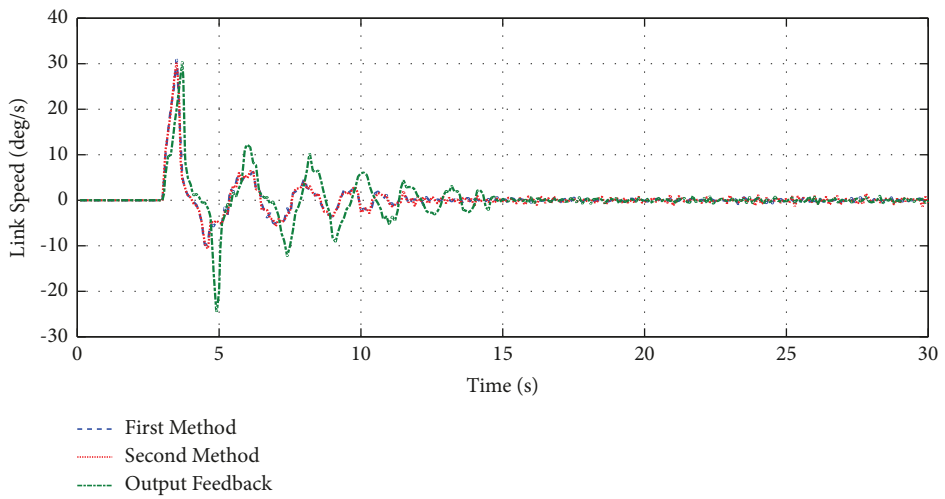

Figure 11: Link speed comparison of both proposed methods with output feedback method.

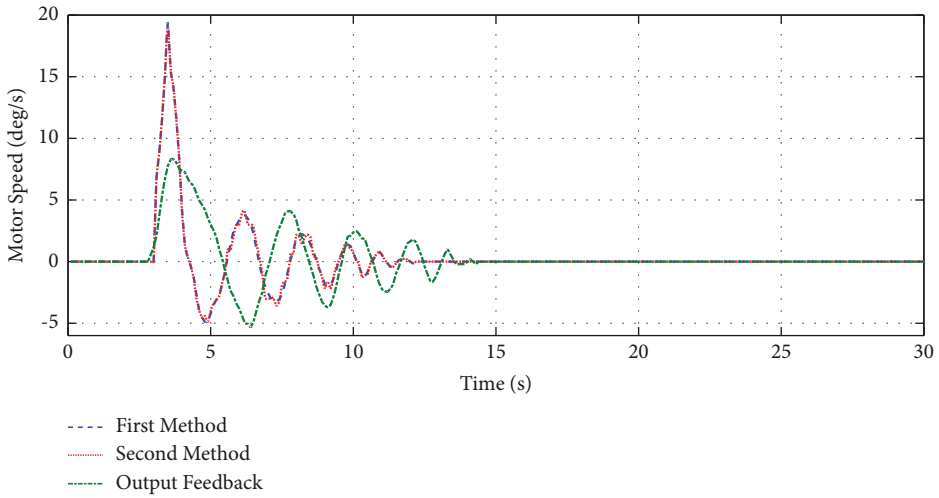

Figure 12: Motor speed comparison of both proposed methods with output feedback method.

Table 2: Comparison of integration of the controller output's area under the curve.

	Integration of controller area in the present method	Integration of controller area in the method of [16]
Controller of robot 1	0.7589	2.9206
Controller of robot 2	0.7178	1.8167
Controller of robot 3	0.3745	2.8942
Controller of robot 4	0.5535	2.2643

Table 3: Parameters of the designed controller and the controller of [16].

Controller type	Designed parameters	Nearest pole to the origin
Designed controller	$A_1 = \begin{pmatrix} -2.61 & 0.001 \\ 0.001 & -2.6103 \end{pmatrix}, B_1 = \begin{pmatrix} 0.0039 & 0.0021 \\ 0.0044 & 0.0025 \end{pmatrix}$ $C_1 = \begin{pmatrix} -0.0023 & -0.0024 \end{pmatrix}, D_1 = \begin{pmatrix} -0.1386 & -0.2013 \end{pmatrix}$ $A_2 = \begin{pmatrix} -2.614 & 0.001 \\ 0.001 & -2.615 \end{pmatrix}, B_2 = \begin{pmatrix} 0.0047 & 0.0024 \\ 0.005 & 0.0026 \end{pmatrix}$ $C_2 = \begin{pmatrix} -0.0027 & -0.0029 \end{pmatrix}, D_2 = \begin{pmatrix} -0.1373 & -0.201 \end{pmatrix}$ $A_3 = \begin{pmatrix} -2.619 & 0.001 \\ 0.001 & -2.603 \end{pmatrix}, B_3 = \begin{pmatrix} 0.004 & 0.0025 \\ 0.0045 & 0.0029 \end{pmatrix}$ $C_3 = \begin{pmatrix} -0.0026 & -0.0029 \end{pmatrix}, D_3 = \begin{pmatrix} -0.138 & -0.201 \end{pmatrix}$	−0.362
Controller of [16]	$K = \begin{pmatrix} -2.762 & 1.885 & -0.32 & -0.341 \end{pmatrix}$	−0.362

Table 4: Comparison of control methods.

Control method	RMSE without uncertainty	RMSE with 20% uncertainty	Settling time (s)	Overshoot (%)
Method of [33]	0.51	0.75	10	37
Method of [44]	0.35	0.62	8	34
Our first method	0.17	0.26	8	19
Our second method	0.16	0.24	7	21

6. Conclusions

In this article, two completely innovative methods for controlling multi-agent systems were introduced. Here, the agents are robots with flexible joints, which is a very challenging problem. A lot of uncertainties, the presence of time delays due to the flexible joint, etc. were among the problems of the studied system. The proposed solution of this article to solve the above problems was to use computing intelligence to estimate functions. The type-2 fuzzy neural network was able to overcome the mentioned challenges and provide a suitable answer both independently and in addition to LMI (As compensator). Both proposed methods work the same and none of them had absolute superiority over the other. By using the proposed method in this article, the challenges related to flexible systems have been solved and time delays have been eliminated. Also, all the states of the system have been measured. In our first method, RMSE without uncertainty, RMSE with 20% uncertainty, Settling time (s), and Overshoot are equal to 0.17, 0.26, 8, and 19%4, respectively, and in our second method, these values are equal to 0.16, 0.24, 7, and 21%, respectively, and in comparison with output feedback method, as shown in the simulation section, it has much better and more suitable results.

Appendix

The update relations of the parameters are as follows:

$$\begin{aligned} e_t &= y_{dt} - \hat{y}_t, \\ E_t &= \frac{1}{2}e_t^2 = \frac{1}{2}\left(y_{dt} - \hat{y}_t\right)^2, \\ E &= \sum_{t=1}^{N} E_t, \end{aligned} \tag{A.1}$$

$$\begin{aligned} {}^{\text{new}}c_{w_i}^1 &= {}^{\text{old}}c_{w_i}^1 + \eta * 0.5 * e_t\left(\frac{\partial \hat{y}}{\partial c_{w_i}^1}\right), \\ {}^{\text{new}}c_{w_i}^2 &= {}^{\text{old}}c_{w_i}^2 + \eta * 0.5 * e_t\left(\frac{\partial \hat{y}}{\partial c_{w_i}^2}\right), \\ {}^{\text{new}}\sigma_{w_i} &= {}^{\text{old}}\sigma_{w_i} + \eta * 0.5 * e_t\left(\frac{\partial \hat{y}}{\partial \sigma_{w_i}}\right), \\ {}^{\text{new}}c_i^1 &= {}^{\text{old}}c_i^1 + \eta * 0.5 * e_t\left(\frac{\partial \hat{y}}{\partial c_i^1}\right), \\ {}^{\text{new}}c_i^2 &= {}^{\text{old}}c_i^2 + \eta * 0.5 * e_t\left(\frac{\partial \hat{y}}{\partial c_i^2}\right), \\ {}^{\text{new}}\sigma_i &= {}^{\text{old}}\sigma_i + \eta * 0.5 * e_t\left(\frac{\partial \hat{y}}{\partial \sigma_i}\right), \end{aligned} \tag{A.2}$$

if $i \le q \,\&\, i \le p$

$$\begin{aligned} \frac{\partial \hat{y}}{\partial c_{w_i}^1} &= \frac{\underline{\varnothing}_i(x)\sigma_{w_i}}{\sum_{i=1}^{p}\underline{\varnothing}_i(x)\sigma_{w_i} + \sum_{i=p+1}^{m}\overline{\varnothing}_i(x)\sigma_{w_i}}, \\ \frac{\partial \hat{y}}{\partial c_{w_i}^2} &= \frac{\overline{\varnothing}_i(x)\sigma_{w_i}}{\sum_{i=1}^{q}\underline{\varnothing}_i(x)\sigma_{w_i} + \sum_{i=q+1}^{m}\overline{\varnothing}_i(x)\sigma_{w_i}}, \\ \frac{\partial \hat{y}}{\partial \sigma_{w_i}} &= \frac{A - B}{\left(\sum_{i=1}^{q}\underline{\varnothing}_i(x)\sigma_{w_i} + \sum_{i=q+1}^{m}\overline{\varnothing}_i(x)\sigma_{w_i}\right)^2} + \frac{C - D}{\left(\sum_{i=1}^{p}\underline{\varnothing}_i(x)\sigma_{w_i} + \sum_{i=p+1}^{m}\overline{\varnothing}_i(x)\sigma_{w_i}\right)^2}, \end{aligned}$$

$$\begin{aligned} A &= \left(\overline{\varnothing}_i(x)c_{w_i}^2\right)\left(\sum_{i=1}^{q}\underline{\varnothing}_i(x)\sigma_{w_i} + \sum_{i=q+1}^{m}\overline{\varnothing}_i(x)\sigma_{w_i}\right), \\ B &= \left(\overline{\varnothing}_i(x)\right)\left(\sum_{i=1}^{q}\overline{\varnothing}_i(x)c_{w_i}^2\sigma_{w_i} + \sum_{i=q+1}^{m}\underline{\varnothing}_i(x)c_{w_i}^1\sigma_{w_i}\right), \\ C &= \left(\underline{\varnothing}_i(x)c_{w_i}^1\right)\left(\sum_{i=1}^{p}\underline{\varnothing}_i(x)\sigma_{w_i} + \sum_{i=p+1}^{m}\overline{\varnothing}_i(x)\sigma_{w_i}\right), \\ D &= \left(\underline{\varnothing}_i(x)\right)\left(\sum_{i=1}^{p}\underline{\varnothing}_i(x)c_{w_i}^1\sigma_{w_i} + \sum_{i=p+1}^{m}\overline{\varnothing}_i(x)c_{w_i}^2\sigma_{w_i}\right), \end{aligned} \tag{A.3}$$

if $i > q \,\&\, i \le p$

$$\frac{\partial \hat{y}}{\partial c_{w_i}^1} = \frac{\underline{\varnothing}_i(x)\sigma_{w_i}}{\sum_{i=1}^{p}\underline{\varnothing}_i(x)\sigma_{w_i} + \sum_{i=p+1}^{m}\overline{\varnothing}_i(x)\sigma_{w_i}} + \frac{\underline{\varnothing}_i(x)\sigma_{w_i}}{\sum_{i=1}^{q}\underline{\varnothing}_i(x)\sigma_{w_i} + \sum_{i=q+1}^{m}\overline{\varnothing}_i(x)\sigma_{w_i}},$$

$$\frac{\partial \hat{y}}{\partial c_{w_i}^2} = 0,$$

$$\frac{\partial \hat{y}}{\partial \sigma_{w_i}} = \frac{A-B}{\left(\sum_{i=1}^{q}\underline{\varnothing}_i(x)\sigma_{w_i} + \sum_{i=q+1}^{m}\overline{\varnothing}_i(x)\sigma_{w_i}\right)^2} + \frac{C-D}{\left(\sum_{i=1}^{p}\underline{\varnothing}_i(x)\sigma_{w_i} + \sum_{i=p+1}^{m}\overline{\varnothing}_i(x)\sigma_{w_i}\right)^2},$$

$$A = \left(\underline{\varnothing}_i(x)c_{w_i}^1\right)\left(\sum_{i=1}^{q}\underline{\varnothing}_i(x)\sigma_{w_i} + \sum_{i=q+1}^{m}\overline{\varnothing}_i(x)\sigma_{w_i}\right), \tag{A.4}$$

$$B = \left(\underline{\varnothing}_i(x)\right)\left(\sum_{i=1}^{q}\overline{\varnothing}_i(x)c_{w_i}^2\sigma_{w_i} + \sum_{i=q+1}^{m}\underline{\varnothing}_i(x)c_{w_i}^1\sigma_{w_i}\right),$$

$$C = \left(\underline{\varnothing}_i(x)c_{w_i}^1\right)\left(\sum_{i=1}^{p}\underline{\varnothing}_i(x)\sigma_{w_i} + \sum_{i=p+1}^{m}\overline{\varnothing}_i(x)\sigma_{w_i}\right),$$

$$D = \left(\underline{\varnothing}_i(x)\right)\left(\sum_{i=1}^{p}\underline{\varnothing}_i(x)c_{w_i}^1\sigma_{w_i} + \sum_{i=p+1}^{m}\overline{\varnothing}_i(x)c_{w_i}^2\sigma_{w_i}\right),$$

if $i > q \,\&\, i > p$

$$\frac{\partial \hat{y}}{\partial c_{w_i}^1} = \frac{\underline{\varnothing}_i(x)\sigma_{w_i}}{\sum_{i=1}^{q}\underline{\varnothing}_i(x)\sigma_{w_i} + \sum_{i=q+1}^{m}\overline{\varnothing}_i(x)\sigma_{w_i}},$$

$$\frac{\partial \hat{y}}{\partial c_{w_i}^2} = \frac{\overline{\varnothing}_i(x)\sigma_{w_i}}{\sum_{i=1}^{p}\underline{\varnothing}_i(x)\sigma_{w_i} + \sum_{i=p+1}^{m}\overline{\varnothing}_i(x)\sigma_{w_i}},$$

$$\frac{\partial \hat{y}}{\partial \sigma_{w_i}} = \frac{A-B}{\left(\sum_{i=1}^{q}\underline{\varnothing}_i(x)\sigma_{w_i} + \sum_{i=q+1}^{m}\overline{\varnothing}_i(x)\sigma_{w_i}\right)^2} + \frac{C-D}{\left(\sum_{i=1}^{p}\underline{\varnothing}_i(x)\sigma_{w_i} + \sum_{i=p+1}^{m}\overline{\varnothing}_i(x)\sigma_{w_i}\right)^2},$$

$$A = \left(\underline{\varnothing}_i(x)c_{w_i}^1\right)\left(\sum_{i=1}^{q}\underline{\varnothing}_i(x)\sigma_{w_i} + \sum_{i=q+1}^{m}\overline{\varnothing}_i(x)\sigma_{w_i}\right), \tag{A.5}$$

$$B = \left(\underline{\varnothing}_i(x)\right)\left(\sum_{i=1}^{q}\overline{\varnothing}_i(x)c_{w_i}^2\sigma_{w_i} + \sum_{i=q+1}^{m}\underline{\varnothing}_i(x)c_{w_i}^1\sigma_{w_i}\right),$$

$$C = \left(\overline{\varnothing}_i(x)c_{w_i}^2\right)\left(\sum_{i=1}^{p}\underline{\varnothing}_i(x)\sigma_{w_i} + \sum_{i=p+1}^{m}\overline{\varnothing}_i(x)\sigma_{w_i}\right),$$

$$D = \left(\overline{\varnothing}_i(x)\right)\left(\sum_{i=1}^{p}\underline{\varnothing}_i(x)c_{w_i}^1\sigma_{w_i} + \sum_{i=p+1}^{m}\overline{\varnothing}_i(x)c_{w_i}^2\sigma_{w_i}\right).$$

The derivative of the network output with respect to the cell parameters of the radial basis function is in the following form. For this purpose, the entrance space must be separated first.

If $i \le q$

$$x_j < c_{ji}^1$$

$$\frac{\partial \hat{y}}{\partial c_{ji}^1} = 2.\frac{c_{w_i}^2 \sigma_{w_i} F - \sigma_{w_i} G}{(F)^2} \frac{\left(x_j - c_{ji}^1\right)}{\sigma_i^2}.\overline{\varnothing}_i(x) \tag{A.6}$$

$$\frac{\partial \hat{y}}{\partial \sigma_i} = 2.\frac{c_{w_i}^2 \sigma_{w_i} F - \sigma_{w_i} G}{(F)^2} \frac{\| x - c_i^1 \|^2}{\sigma_i^3}.\overline{\varnothing}_i(x)$$

$$x_j > c_{ji}^2$$

$$\frac{\partial \hat{y}}{\partial c_{ji}^2} = 2.\frac{c_{w_i}^2 \sigma_{w_i} F - \sigma_{w_i} G}{(F)^2} \frac{\left(x_j - c_{ji}^2\right)}{\sigma_i^2}.\overline{\varnothing}_i(x) \tag{A.7}$$

$$\frac{\partial \hat{y}}{\partial \sigma_i} = 2.\frac{c_{w_i}^2 \sigma_{w_i} F - \sigma_{w_i} G}{(F)^2} \frac{\| x - c_i^2 \|^2}{\sigma_i^3}.\overline{\varnothing}_i(x)$$

where in

$$F = \sum_{i=1}^{q} \overline{\varnothing}_i(x) \sigma_{w_i}$$
$$G = \sum_{i=1}^{q} \overline{\varnothing}_i(x) c_{w_i}^2 \sigma_{w_i} \tag{A.8}$$

if $i > q$

$$x_j > \frac{c_{ji}^1 + c_{ji}^2}{2}$$

$$\frac{\partial \hat{y}}{\partial c_i^1} = 2.\frac{c_{w_i}^1 \sigma_{w_i} H - \sigma_{w_i} Y}{(H)^2} \frac{\left(x_j - c_{ji}^1\right)}{\sigma_i^2}.\underline{\varnothing}_i(x)$$

$$\frac{\partial \hat{y}}{\partial \sigma_i} = 2.\frac{c_{w_i}^1 \sigma_{w_i} H - \sigma_{w_i} Y}{(H)^2} \frac{\| x - c_i^1 \|^2}{\sigma_i^3}.\underline{\varnothing}_i(x) \tag{A.9}$$

$$\text{where in } Y = \sum_{i=q+1}^{m} \underline{\varnothing}_i(x) c_{w_i}^1 \sigma_{w_i}$$

$$H = \sum_{i=q+1}^{m} \underline{\varnothing}_i(x) \sigma_{w_i}$$

if $i \le p$

$$x_j \le \frac{c_{ji}^1 + c_{ji}^2}{2}$$

$$\frac{\partial \hat{y}}{\partial c_{ji}^2} = 2.\frac{c_{w_i}^1 \sigma_{w_i} K - \sigma_{w_i} L}{(K)^2} \frac{\left(x_j - c_{ji}^2\right)}{\sigma_i^2}.\underline{\varnothing}_i(x) \tag{A.10}$$

$$\frac{\partial \hat{y}}{\partial \sigma_i} = 2.\frac{c_{w_i}^1 \sigma_{w_i} K - \sigma_{w_i} L}{(K)^2} \frac{\| x - c_i^2 \|^2}{\sigma_i^3}.\underline{\varnothing}_i(x)$$

$$x_j > \frac{c_{ji}^1 + c_{ji}^2}{2}$$

$$\frac{\partial \hat{y}}{\partial c_{ji}^1} = 2.\frac{c_{w_i}^1 \sigma_{w_i} K - \sigma_{w_i} L}{(K)^2} \frac{\left(x_j - c_{ji}^1\right)}{\sigma_i^2}.\underline{\varnothing}_i(x)$$

$$\frac{\partial \hat{y}}{\partial \sigma_i} = 2.\frac{c_{w_i}^1 \sigma_{w_i} K - \sigma_{w_i} L}{(K)^2} \frac{\| x - c_i^1 \|^2}{\sigma_i^3}.\underline{\varnothing}_i(x)$$

$$\text{where in } L = \sum_{i=1}^{p} \underline{\varnothing}_i(x) c_{w_i}^1 \sigma_{w_i}$$

$$K = \sum_{i=1}^{p} \underline{\varnothing}_i(x) \sigma_{w_i} \tag{A.11}$$

if $i > p$

$$x_j < c_{ji}^1$$

$$\frac{\partial \hat{y}}{\partial c_{ji}^1} = 2.\frac{c_{w_i}^2 \sigma_{w_i} Z - \sigma_{w_i} R}{(Z)^2} \frac{\left(u_j - c_{ji}^1\right)}{\sigma_i^2}.\overline{\varnothing}_i(u) \tag{A.12}$$

$$\frac{\partial \hat{y}}{\partial \sigma_i} = 2.\frac{c_{w_i}^2 \sigma_{w_i} Z - \sigma_{w_i} R}{(Z)^2} \frac{\| u - c_i^1 \|^2}{\sigma_i^3}.\overline{\varnothing}_i(u)$$

$$x_j > c_{ji}^2$$

$$\frac{\partial \hat{y}}{\partial c_{ji}^2} = 2.\frac{c_{w_i}^2 \sigma_{w_i} Z - \sigma_{w_i} R}{(Z)^2} \frac{\left(u_j - c_{ji}^2\right)}{\sigma_i^2}.\overline{\varnothing}_i(u)$$

$$\frac{\partial \hat{y}}{\partial \sigma_i} = 2.\frac{c_{w_i}^2 \sigma_{w_i} Z - \sigma_{w_i} R}{(Z)^2} \frac{\| u - c_i^2 \|^2}{\sigma_i^3}.\overline{\varnothing}_i(u)$$

$$\text{where in } R = \sum_{i=p+1}^{m} \overline{\varnothing}_i(u) c_{w_i}^2 \sigma_{w_i}$$

$$Z = \sum_{i=p+1}^{m} \overline{\varnothing}_i(u) \sigma_{w_i} \tag{A.13}$$

Data Availability

No underlying data were collected or produced in this study.

Conflicts of Interest

The authors declare that they have no conflicts of interest.

Acknowledgments

This research study was funded by the Scientific Research Foundation of Hunan Provincial Education Department (20C0561)—Research on prediction method of the relationship between microorganism and disease based on data fusion.

References

[1] F. N. Abd Latiff and W. A. Mior Othman, "Results for chaos synchronization with new multi-fractional order of neural networks by multi-time delay," *Complexity*, vol. 2021, Article ID 9398333, pp. 1–17, 2021.

[2] Y. Li, C. Li, L. You, Z. He, and H. Li, "Exponential synchronisation of nonlinear multi-agent systems via distributed self-triggered hybrid control with virtual linked agents," *International Journal of Control*, vol. 95, no. 12, pp. 3241–3251, 2021.

[3] H. Huang, M. Shirkhani, J. Tavoosi, and O. Mahmoud, "A new intelligent dynamic control method for a class of stochastic nonlinear systems," *Mathematics*, vol. 10, no. 9, p. 1406, 2022.

[4] J. G. Lee, S. Trenn, and H. Shim, "Synchronization with prescribed transient behavior: heterogeneous multi-agent systems under funnel coupling," *Automatica*, vol. 141, 2022.

[5] C. Cao, J. Wang, D. Kwok et al., "webTWAS: a resource for disease candidate susceptibility genes identified by transcriptome-wide association study," *Nucleic Acids Research*, vol. 50, no. D1, pp. D1123–D1130, 2022.

[6] Y. Fan, X. Ren, and Z. Li, "Distributed adaptive neural network control for a class of uncertain heterogeneous multi-agent systems," *International Journal of Innovative Computing, Information and Control*, vol. 18, no. 1, pp. 289–304, 2022.

[7] H. Zhao, N. Zhao, G. Zong, X. Zhao, and N. Xu, "Sliding-mode surface-based approximate optimal control for nonlinear multiplayer Stackelberg-Nash games via adaptive dynamic programming," *Communications in Nonlinear Science and Numerical Simulation*, vol. 20, 2024.

[8] C. Deeks, "Adapting multi-agent swarm robotics to achieve synchronised behaviour from production line automata," *Springer Proceedings in Advanced Robotics*, pp. 13–24, Springer International Publishing, New York, NY, USA, 2022.

[9] S. Huang, B. Niu, H. Wang, N. Xu, and X. Zhao, "Prescribed performance-based low-complexity adaptive 2-bit-triggered control for unknown nonlinear systems with actuator deadzone," *IEEE Transactions on Circuits and Systems II: Express Briefs*, vol. 71, no. 2, pp. 762–766, 2024.

[10] K. C. Chen and H. M. Hung, "Wireless robotic communication for collaborative multi-agent systems," in *Proceedings of the ICC 2019- 2019 IEEE International Conference on Communications (ICC)*, pp. 1–7, Shanghai, China, May 2019.

[11] Z. Gao, N. Zhao, X. Zhao, B. Niu, and N. Xu, "Event-triggered prescribed performance adaptive secure control for nonlinear cyber physical systems under denial-of-service attacks," *Communications in Nonlinear Science and Numerical Simulation*, vol. 131, 2024.

[12] S. Ling, H. Wang, and P. X. Liu, "Adaptive fuzzy dynamic surface control of flexible-joint robot systems with input saturation," *IEEE/CAA Journal of Automatica Sinica*, vol. 6, no. 1, pp. 97–107, 2019.

[13] S. Liu, B. Niu, N. Xu, and X. Zhao, "Zero-sum game-based decentralized optimal control for saturated nonlinear interconnected systems via a data and event driven approach," *IEEE Systems Journal*, vol. 18, no. 1, pp. 758–769, 2024.

[14] P. Zhou, P. Zheng, J. Qi et al., "Reactive human–robot collaborative manipulation of deformable linear objects using a new topological latent control model," *Robotics and Computer-Integrated Manufacturing*, vol. 88, 2024.

[15] S. Ling, H. Wang, and P. X. Liu, "Adaptive fuzzy tracking control of flexible-joint robots based on command filtering," *IEEE Transactions on Industrial Electronics*, vol. 67, no. 5, pp. 4046–4055, 2020.

[16] R. Aazami, M. Shoaei, A. Moradkhani, M. Shirkhani, A. Elrashidi, and K. M. AboRas, "Deep neural networks based method to islanding detection for multi-sources microgrid," *Energy Reports*, vol. 11, pp. 2971–2982, 2024.

[17] J. Yu, X. Dong, Q. Li, J. Lü, and Z. Ren, "Adaptive practical optimal time-varying formation tracking control for disturbed high-order multi-agent systems," *IEEE Transactions on Circuits and Systems I: Regular Papers*, vol. 69, no. 6, pp. 2567–2578, 2022.

[18] Y. T. dos Passos, X. Duquesne, and L. S. Marcolino, "On the throughput of the common target area for robotic swarm strategies," *Mathematics*, vol. 10, no. 14, p. 2482, 2022.

[19] B. Ma, Z. Liu, Q. Dang et al., "Deep reinforcement learning of UAV tracking control under wind disturbances environments," *IEEE Transactions on Instrumentation and Measurement*, vol. 72, pp. 1–13, 2023.

[20] R. Aazami, S. Dabestani, and M. Shirkhani, "Optimal capacity and location for renewable-based microgrids considering economic planning in distribution networks," *International Journal of Engineering*, vol. 36, no. 12, pp. 2175–2183, 2023.

[21] K. Li, L. Ji, S. Yang, H. Li, and X. Liao, "Couple-group consensus of cooperative–competitive heterogeneous multi-agent systems: a fully distributed event-triggered and pinning control method," *IEEE Transactions on Cybernetics*, vol. 52, no. 6, pp. 4907–4915, 2022.

[22] A. Zhang, Z. Lin, B. Wang, and Z. Han, "Nonlinear model predictive control of single-link flexible-joint robot using recurrent neural network and differential evolution optimization," *Electronics*, vol. 10, no. 19, p. 2426, 2021.

[23] A. B. Dawood, J. Fras, F. Aljaber et al., "Fusing dexterity and perception for soft robot-assisted minimally invasive surgery: what we learnt from STIFF-FLOP," *Applied Sciences*, vol. 11, no. 14, p. 6586, 2021.

[24] Y. Liu, Z. Li, H. Su, L. Jiang, and C. Y. Su, "Whole body control of an autonomous mobile manipulator using series elastic actuators," *IEEE*, p. 1, 2024.

[25] S. Chen and J. T. Wen, "Adaptive neural trajectory tracking control for flexible-joint robots with online learning," in *Proceedings of the 2020 IEEE International Conference on Robotics and Automation (ICRA)*, pp. 2358–2364, Paris, France, May 2020.

[26] T. Hao, H. Wang, F. Xu, J. Wang, and Y. Miao, "Uncalibrated visual servoing for a planar two link rigid-flexible manipulator without joint-space-velocity measurement," *IEEE Transactions on Systems, Man, and Cybernetics: Systems*, vol. 52, no. 3, pp. 1935–1947, 2022.

[27] X. Liang, Z. Chen, Y. Deng et al., "Field-controlled microrobots fabricated by photopolymerization," *Cyborg and Bionic Systems*, vol. 4, p. 0009, 2023.

[28] S. A. Zimmermann, T. F. Berninger, J. Derkx, and D. J. Rixen, "Dynamic modeling of robotic manipulators for accuracy evaluation," in *Proceedings of the 2020 IEEE International Conference on Robotics and Automation (ICRA)*, pp. 8144–8150, Paris, France, May 2020.

[29] H. Zhang, Q. Zou, Y. Ju, C. Song, and D. Chen, "Distance-based support vector machine to predict DNA N6-methyladenine modification," *Current Bioinformatics*, vol. 17, no. 5, pp. 473–482, 2022.

[30] S. Danyali, A. Moradkhani, O. Abdulhussein Abdaumran, M. Shirkhani, and Z. Dadvand, "A novel multi-input medium-gain DC-DC boost converter with soft-switching performance," *International Journal of Electrical Power & Energy Systems*, vol. 155, 2024.

[31] J. Jung, R. S. Penning, N. J. Ferrier, and M. R. Zinn, "A modeling approach for continuum robotic manipulators: effects of nonlinear internal device friction," in *Proceedings of the 2011 IEEE/RSJ International Conference on Intelligent Robots and Systems*, pp. 5139–5146, San Francisco, CA, USA, September 2011.

[32] T. S. Lee and E. A. Alandoli, "A critical review of modelling methods for flexible and rigid link manipulators," *Journal of the Brazilian Society of Mechanical Sciences and Engineering*, vol. 42, no. 10, pp. 508–514, 2020.

[33] X. Li, H. Zhou, S. Zhang, H. Feng, and Y. Fu, "WLR-II, a hoseless hydraulic wheel-legged robot," in *Proceedings of the 2019 IEEE/RSJ International Conference on Intelligent Robots and Systems (IROS)*, pp. 4339–4346, Macau, China, November 2019.

[34] X. Guo, M. Shirkhani, and E. M. Ahmed, "Machine-learning-based improved smith predictive control for MIMO processes," *Mathematics*, vol. 10, no. 19, p. 3696, 2022.

[35] S. Jin, W. Lian, C. Wang, M. Tomizuka, and S. Schaal, "Robotic cable routing with spatial representation," *IEEE Robotics and Automation Letters*, vol. 7, no. 2, pp. 5687–5694, 2022.

[36] S. Danyali, M. Shirkhani, J. Tavoosi, A. G. Razi, M. M. Salah, and A. Shaker, "Developing an integrated soft-switching bi-directional DC/DC converter for solar-powered LED street lighting," *Sustainability*, vol. 15, no. 20, 2023.

[37] T. Klamt, M. Schwarz, C. Lenz et al., "Remote mobile manipulation with the centauro robot: full-body telepresence and autonomous operator assistance," *Journal of Field Robotics*, vol. 37, no. 5, pp. 889–919, 2020.

[38] J. Tavoosi, M. Shirkhani, A. Azizi, S. Ud Din, A. Mohammadzadeh, and S. Mobayen, "A hybrid approach for fault location in power distributed networks: impedance-based and machine learning technique," *Electric Power Systems Research*, vol. 210, 2022.

[39] M. Hadi Barhaghtalab, V. Meigoli, M. R. Golbahar Haghighi, S. A. Nayeri, and A. Ebrahimi, "Dynamic analysis, simulation, and control of a 6-DOF IRB-120 robot manipulator using sliding mode control and boundary layer method," *Journal of Central South University*, vol. 25, no. 9, pp. 2219–2244, 2018.

[40] F. Alambeigi, Z. Wang, R. Hegeman, Y. H. Liu, and M. Armand, "Autonomous data-driven manipulation of unknown anisotropic deformable tissues using unmodelled continuum manipulators," *IEEE Robotics and Automation Letters*, vol. 4, no. 2, pp. 254–261, 2019.

[41] Y. Tian, Y. Guo, and Y. Ji, "Consensus in discrete-time one-sided Lipschitz nonlinear multi-agent systems with time-varying communication delay," *European Journal of Control*, vol. 65, 2022.

[42] D. Chen, X. Liu, and W. Yu, "Finite-time fuzzy adaptive consensus for heterogeneous nonlinear multi-agent systems," *IEEE Transactions on Network Science and Engineering*, vol. 7, no. 4, pp. 3057–3066, 2020.

[43] A. Amirkhani and A. H. Barshooi, "Consensus in multi-agent systems: a review," *Artificial Intelligence Review*, vol. 55, no. 5, pp. 3897–3935, 2021.

[44] Y. M. Li, K. Li, and S. Tong, "An observer-based fuzzy adaptive consensus control method for nonlinear multi-agent systems," *IEEE Transactions on Fuzzy Systems*, vol. 30, no. 11, pp. 4667–4678, 2022.

[45] H. Zhou, S. Cao, S. Zhang, F. Li, and N. Ma, "Design of a fuel explosion-based chameleon-like soft robot aided by the comprehensive dynamic model," *Cyborg and Bionic Systems*, vol. 4, p. 0010, 2023.

[46] S. Danyali, O. Aghaei, M. Shirkhani et al., "A new model predictive control method for buck-boost inverter-based photovoltaic systems," *Sustainability*, vol. 14, no. 18, p. 11731, 2022.

[47] A. Azizi, J. Tavoosi, and M. Shirkhani, "Control engineering solutions during epidemics: a review," *International Journal of Modelling, Identification and Control*, vol. 39, no. 2, pp. 97–106, 2021.

[48] C. Guo and J. Hu, "Time base generator based practical predefined-time stabilization of high-order systems with unknown disturbance," *IEEE Transactions on Circuits and Systems II: Express Briefs*, vol. 70, no. 7, pp. 2670–2674, 2023.

[49] M. R. Jafari, M. M. Arefi, and M. Panahi, "Convex reformulations for self-optimizing control optimization problem: linear Matrix Inequality approach," *Journal of Process Control*, vol. 116, pp. 172–184, 2022.

[50] Y. Sun, Z. Peng, J. Hu, and B. K. Ghosh, "Event-triggered critic learning impedance control of lower limb exoskeleton robots in interactive environments," *Neurocomputing*, vol. 564, 2024.

[51] B. Chen, J. Hu, Y. Zhao, and B. K. Ghosh, "Finite-time observer based tracking control of uncertain heterogeneous underwater vehicles using adaptive sliding mode approach," *Neurocomputing*, vol. 481, pp. 322–332, 2022.

[52] W. Y. Chiu, "Method of reduction of variables for bilinear matrix inequality problems in system and control designs," *IEEE Transactions on Systems, Man, and Cybernetics: Systems*, vol. 47, no. 7, pp. 1241–1256, 2017.

[53] G. Wen, Z. Duan, G. Chen, and W. Yu, "Consensus tracking of multi-agent systems with Lipschitz-type node dynamics and switching topologies," *IEEE Transactions on Circuits and Systems I: Regular Papers*, vol. 61, no. 2, pp. 499–511, 2014.

[54] S. Alves, M. Babcinschi, A. Silva, D. Neto, D. Fonseca, and P. Neto, "Integrated design fabrication and control of a bio-inspired multimaterial soft robotic hand," *Cyborg and Bionic Systems*, vol. 4, p. 0051, 2023.

[55] Y. Wang, H. Chen, J. Law, X. Du, and J. Yu, "Ultrafast miniature robotic swimmers with upstream motility," *Cyborg and Bionic Systems*, vol. 4, p. 15, 2023.

[56] X. Li, H. Yu, H. Feng, S. Zhang, and Y. Fu, "Design and control for WLR-3P: a hydraulic wheel-legged robot," *Cyborg and Bionic Systems*, vol. 4, p. 25, 2023.

[57] Y. Wang, E. Garcia, D. Casbeer, and F. Zhang, Eds., *Cooperative Control of Multi-Agent Systems: Theory and Applications*, Wiley, Hoboken, NJ, USA, 2023.

[58] J. Qu, B. Mao, Z. Li et al., "Recent progress in advanced tactile sensing technologies for soft grippers," *Advanced Functional Materials*, vol. 33, no. 41, 2023.
[59] R. Merris, "Laplacian matrices of graphs: a survey," *Linear Algebra and its Applications*, vol. 197-198, pp. 143–176, 1994.
[60] D. Khan, M. Alonazi, M. Abdelhaq et al., "Robust human locomotion and localization activity recognition over multisensory," *Frontiers in Physiology*, vol. 15, 2024.
[61] S. Zhang, F. Li, R. Fu et al., "A versatile continuum gripping robot with a concealable gripper," *Cyborg and Bionic Systems*, vol. 4, p. 3, 2023.
[62] M. S. Hesarian and J. Tavoosi, "Evaluating the Smoothness of the Washed Fabric after Laundry with the Washing Machine Based on a New Type-2 Fuzzy Neural Network," *Complexity*, vol. 2022, Article ID 2401736, p. 9, 2022.